

Bamboo-precocious wood composite beams: bending capacity for long-term loading

Y. AMINO *

*Structural Design and Timber Engineering, Institute of Architectural Sciences,
Vienna University of Technology, Karlsplatz 13/259, A-1040 Vienna, Austria*

Abstract—Similar to timbers, bamboo shows creep behaviour under sustained load. However, a remarkable performance is shown during static experiments, the degradation of the performance by the creep must be discussed to secure the utilization over a long period. In order to study the long-term efficiency of bamboo laminas reinforcing low-quality precocious wood beams, a series of creep tests was carried out on two types of specimens: bamboo–poplar sandwich beams and non-reinforced poplar beams. Under a constant climatic condition, the load on the beams was stepwise increased to observe the behaviour at different load levels. Analyzing the experimental data of the sandwich beams, the long-term admissible load level, as well as the supplemental deformation was studied. In accordance with the Burger body model, their behaviour was analytically interpreted in order to obtain the coefficients characterizing the creep curves. Comparing these coefficients revealed the influence of bamboo reinforcement on the creep.

Key words: Composite; sandwich beam; bamboo; precocious wood; poplar; reinforcement; creep; Burger body.

INTRODUCTION

For the proposed bamboo–poplar sandwich beams, the bending properties under the static loading were discussed in the previous study [1, 2] and the efficiency of bamboo reinforcement was revealed without regard to the duration of loading. However, real beams are used under long-term loading. The initial deflection developed with the load application does not remain constant but increases with time. Numerous examples can be cited in which the time-dependent behaviour of wood is particularly important. The mechanical performance under long-term loading determines the practical loading capacity of timber beams. It is also known that the increase of the additional deflection depends on the climatic condition

*E-mail: y.amino@iti.tuwien.ac.at

surrounding timber beams. High temperature and high humidity amplify the time-dependent deflection increase. As for the growing districts of bamboo and poplar, these are mainly located between the temperate and the torrid zones. Regarding the utilization of the proposed bamboo–poplar sandwich beams in these districts, the study on the time-dependent behaviour under high temperature with high humidity is indispensable.

The experiments reported in this paper were planned to study the characteristics of the loading capacity of the sandwich beams due to the duration of loading under a constant climatic condition. In addition to the sandwich beams, non-reinforced poplar beams were also tested under the same condition. The applied load level was stepwise changed to study the correlation between the creep progression and the different load levels. Even if the given load level is very low, creep deflection takes place, but the increase of the deflection stops with the passage of time. When the load exceeds a certain level inherent for the material, called the creep limit, the deflection increases progressively until the beam ruptures. Obtaining this load level is important for the beam design. The creep limit determinates the long-term admissible load on the beam.

After determining the creep limit, the creep curves were analyzed on the basis of a generalized theoretical model consisting of two Hookean springs and two Newtonian dashpots. The combination of these elements represents an analogy of the creep deformation. The model interprets the deflection evolution of the bamboo–poplar beam, computing the inherent parameters of the specimens.

MATERIALS AND METHODS

Specimens

Nine bamboo–poplar sandwich beams and five non-reinforced poplar beams were prepared for the bending creep tests. Figure 1 illustrates the cross section of these

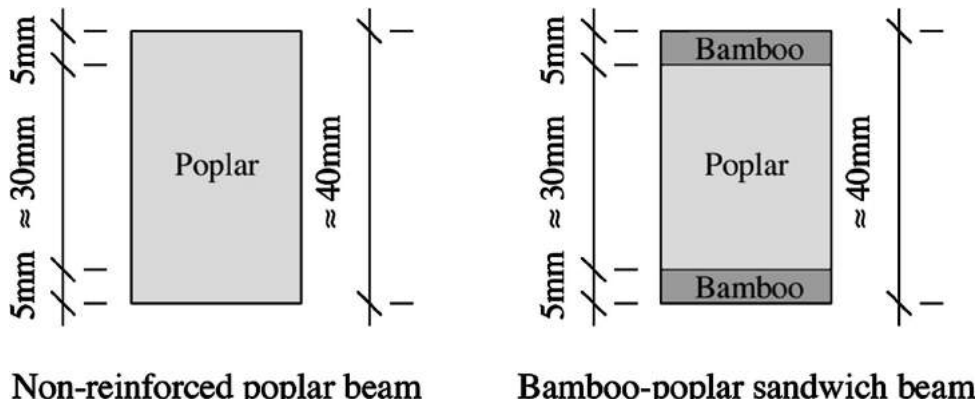


Figure 1. Cross-section of the specimens for the bending creep tests.

Table 1.

Dimensions and MoE of the specimens for the bending creep tests (measured at 20°C and 60% relative humidity)

		Actual dimensions (mm)		Span (mm)	MoE of components (kN/mm ²)		
		Height	Width		Top facing	Core	Bottom facing
Poplar beam	1	40.1	26.1	720	—	6.961	—
	2	40.1	26.1	720	—	7.592	—
	3	40.1	26.1	720	—	7.808	—
	4	40.1	26.1	720	—	8.655	—
	5	40.1	26.1	720	—	9.281	—
Sandwich beam	1st series	1	40.1	26.1	720	9.808	6.839 9.839
	2	40.1	26.1	720	10.090	7.545	10.222
	3	40.1	26.1	720	10.637	7.927	10.836
	4	40.1	26.1	720	11.065	8.551	11.342
	5	40.1	26.1	720	12.141	9.260	12.210
	2nd series	6	40.1	26.1	720	10.755	9.187 10.828
	7	40.1	26.1	720	11.011	8.841	11.281
	8	40.1	26.1	720	11.956	6.716	11.958
	9	40.1	26.1	720	11.991	6.567	12.023

beams. The reinforcement of these beams was chosen from the same lot of Moso bamboo laminas used for the prior static bending tests [1, 2]. All the bamboo layers and poplar beams were graded in accordance with their MoE (Modulus of Elasticity). The reinforcement laminas were fixed on the top and bottom of poplar beams by epoxy resin adhesive. The exact dimensions and MoE of the specimens are given in Table 1.

The room condition during the preparation and grading of the specimens was 20°C in temperature and 60% relative humidity (RH). Under this condition, the average moisture content of the poplar beams was 12.4%. Afterward all the specimens were moved into the test room where constant atmospheric conditions were maintained by the machine air-conditioning. The specimens were kept in this testing condition (25°C, 80% RH) during six weeks at least before the tests in order to stabilize the temperature and moisture content of the materials under the testing condition. The weight of the specimens was periodically measured until the variation disappeared. The average moisture content of the poplar increased to 15.5%. The moisture content of bamboo was ignored, since we paid scant attention to the relationship between the moisture content of the reinforcement and creep behaviour.

Testing device

The device used for the bending creep tests is schematically illustrated in Fig. 2. The test assembly was built inside the air-conditioned room. Each specimen was placed horizontally on the two supporting points of the device. The distance between the

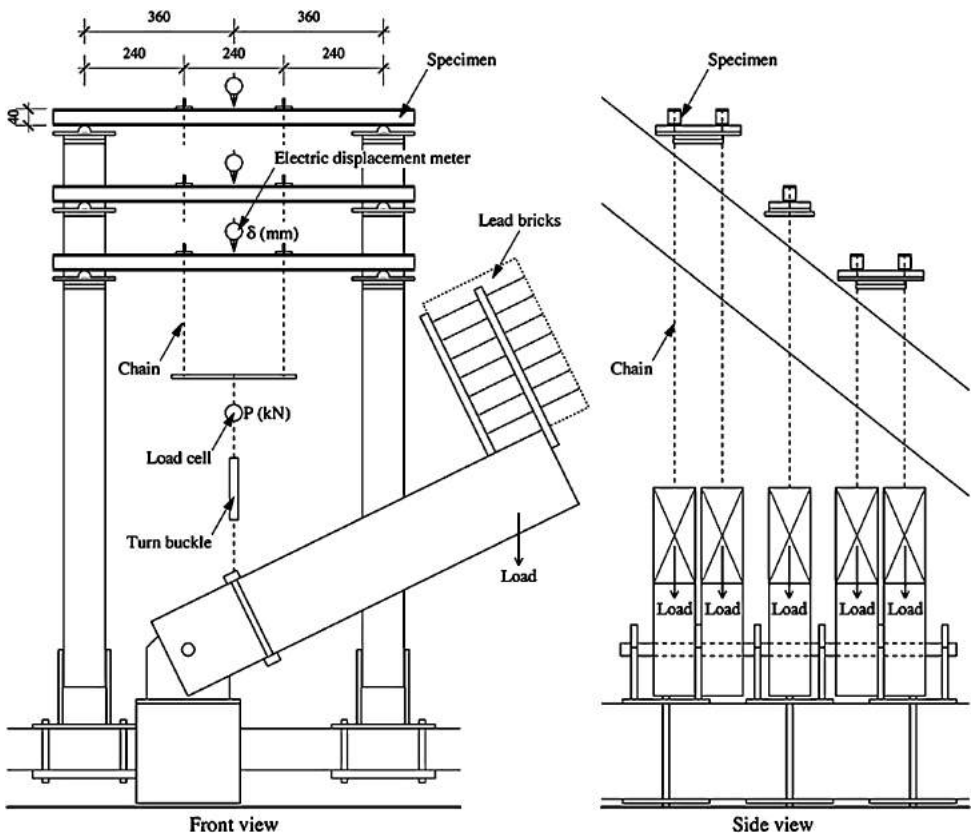


Figure 2. Bending creep testing device.

supporting points was 720 mm. A symmetrical load was applied at the third-points of the specimens. At the supporting points and at the loading points, flat steel plates protected the surfaces of the specimens in order to minimize the perpendicular-to-grain crushing. The loads were applied through the chains stretched between the specimens and the levers located underneath. Each lever carried lead bricks at the free end. By changing the number of bricks, the applied load level was adjusted. The levers amplified and transmitted the load to the chains. The amount of applied load changes due to the rotation of the lever. In order to measure the actual load level, a load cell was fixed between each specimen and lever. An electric displacement meter attached at the span centre measured the bending deflection of each specimen. A sensor also monitored the temperature and humidity of the test room.

Loading condition

In order to obtain a relationship between the creep deformation and the different load levels by testing a limited number of specimens, the load level was increased

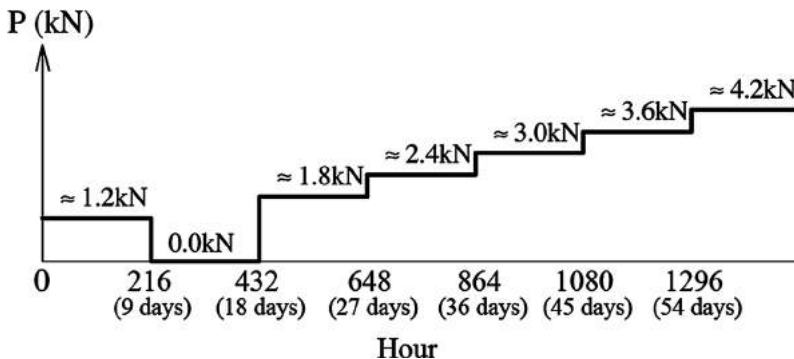


Figure 3. Loading condition of the creep tests.

in steps. The appropriateness of this loading method, non-linear viscoelastic superposition, was studied by Mukudai and Taguchi [3]. The loading schedule is presented in Fig. 3. The duration of a load level was decided to be 9 days (216 h) according to the Japanese norm JIS Z2101 [4]. This norm defines that the minimal duration for the creep test must be 200 h. Note that the load values shown in Fig. 3 are approximate ones and slightly different from the actual values measured by the load cells. This experiment was carried out under constant atmospheric conditions (25°C, 80% RH).

For the first step of loading, about 1.2 kN weight was applied on every specimen. The third-points carried half of it, i.e., 0.6 kN. After 9 days, the specimens were unloaded. Following the first loading, the specimens were kept unloaded for three days, and the recovery of the deflection was measured. When the recovery is not complete, the residual deflection resulted from the creep is named the permanent deflection or the viscous deflection. Measuring the permanent deflection is needed to determine the parameters of the four elements creep model known as the Burger body.

After the period of recovery, the specimens were again loaded with about 1.8 kN weight. At the second loading and after, the load was stepwise increased. About 0.6 kN weight was added every 9 days until the rupture of the specimens.

Generally, to compare the creep behaviour of different materials, the applied loads must be proportional to the static strength of each material. In this study, the same loading condition was applied to both types of beams because of the specificity of the testing device. Since the minimal load by this device was about 1.2 kN, we could not reduce the load for the poplar beams.

RESULTS AND DISCUSSION

Deflection-load-time correlation

Figures 4 and 5 show the typical test results on the poplar beams and on the sandwich beams, respectively. These diagrams illustrate the deflection evolving

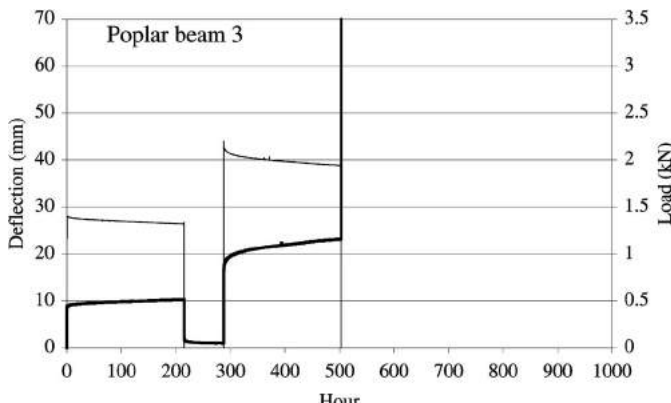


Figure 4. Typical deflection–load–time correlation of the poplar beams.

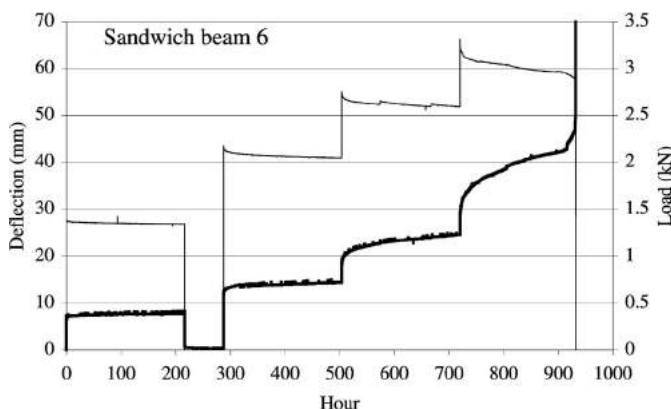


Figure 5. Typical deflection–load–time correlation of the sandwich beams.

with the variation and duration of load. The bold curves represent the deflection–time correlation while the thin curves show the load–time correlation.

As for the poplar beams, all the specimens except one beam failed soon after the third load was applied. Among 9 sandwich beams, 3 specimens failed during the fourth loading. The most resisting specimen bore the fourth loading and failed at the beginning of the fifth loading. The other pieces failed at the beginning or in the middle of the third loading. The results show an improvement of creep bending strength by the bamboo reinforcement. Note that this comparison does not mean the increase of the proportion of loading capacity to the static bending strength.

Admissible load level for long-term loading

From the application of load to the failure, the creep deformation increases inconstantly. It is generally recognized that a creep curve consists of three successive stages: primary, secondary and tertiary. These steps are different from each other in creep rate defined as the speed of deformation increase $d\delta/dt$. The

primary creep shows the creep rate $d\delta/dt$ decreasing. The secondary creep indicates the region, following the primary creep, in which the creep evolution is linear ($d\delta/dt = \text{constant}$). Succeeding the secondary creep, the rate $d\delta/dt$ increases in the tertiary creep region. Tertiary creep finally attains the failure.

The secondary creep can be considered as a transitional condition between the primary and tertiary creep. When the rate $d\delta/dt$ is positive constant, the creep deformation increases linearly until the tertiary creep starts to develop. While the load is under a certain level, the secondary creep does not take place ($d\delta/dt = 0$). Once the deformation increase disappears, the creep is stabilized. In this case, the failure will not be caused by the creep progress. The load level under which the secondary creep does not appear is called the creep limit. Obtaining the creep limit is indispensable to define the admissible load level that assures the long-term loading without failure. Analyzing the creep curves, the creep rates $d\delta/dt$ of the tested specimens can be obtained as the slope of regression lines about their secondary stages.

$$\delta = \left(\frac{d\delta}{dt} \right) t + c. \quad (1)$$

Since the beginning of the secondary stage could not be clearly distinguished, the duration of the secondary creep was supposed uniformly for every specimen: 100 h from the 100th hour after the load application or after the load addition. Figure 6 presents the example of a tested sandwich beam (the same beam in Fig. 5). The load level for each creep rate is also expressed as the form of the stress ratio (S.R.) meaning the proportion of the applied load to the static bending strength. A series of prior static bending tests obtained the referential bending strength: 4.17 kN for the poplar beams and 5.32 kN for the sandwich beams. Note that these referential loads were measured at 60% RH. Under this condition, the water content of poplar was about 12%, which is lower than that of the specimens for the creep tests. On the other hand, the specimens subjected to the creep tests had moisture content of about 15.5%. In this study, the stress ratio means the relation of the creep test load to the static bending strength in the usual room condition.

At the first loading, the average creep rate of the poplar beams was 0.0049 mm/h (average load = 1.31 kN), while the rate of the sandwich beams was 0.0010 mm/h (average load = 1.33 kN). The speed of creep progress was decreased to one fifth by the bamboo reinforcement. At the second loading, the average creep rate was 0.0173 mm/h (average load = 1.89 kN) for the poplar beams and 0.0064 mm/h (average load = 1.95 kN) for the sandwich beams. The bamboo reinforcement showed the efficiency to diminish the creep rate, though the decrease of the rate was smaller than that of the first loading.

From the nine tested sandwich beams, the relationship between the creep rate and the stress ratio is illustrated in Fig. 7. By means of the linear regression about all

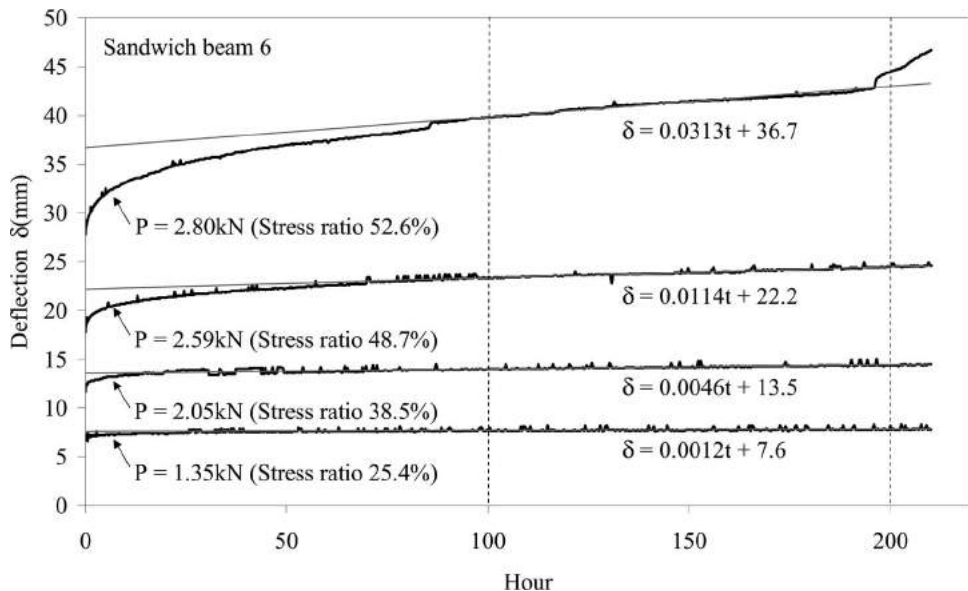


Figure 6. Creep curves evolving with the increase of stress ratio (sandwich beam 6 in Fig. 5).

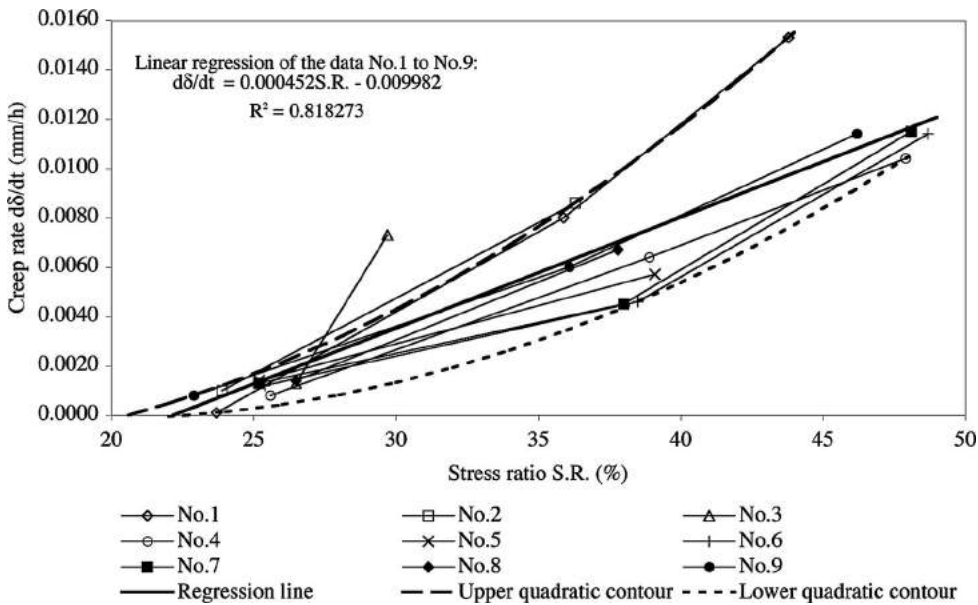


Figure 7. Relationship between the creep rate and the stress ratio (9 sandwich beams).

plotted points in Fig. 7, the creep limit of these beams is approximately given as the intersection of the regression line and the x -axis:

$$\text{Creep limit} \approx 1.18 \text{ kN} \approx 22.1\% \text{ (in S.R.)}.$$

The long-term admissible stress ratio of the tested beams can be found around this value.

Though it is too premature and not our objective to discuss the curve fitting on the obtained data from the insufficient number of specimens, the contours of the points distribution were traced on trial by two quadratic functions, in addition to the above linear regression line. Each quadratic curve passes three points situated around the contour and forms a part of envelope enclosing the points. The quadratic contours are described by the following equations:

$$\text{Upper quadratic contour: } \frac{d\delta}{dt} = 0.00001489(\text{S.R.})^2 - 0.00029952(\text{S.R.}) - 0.00015054,$$

$$\text{Lower quadratic contour: } \frac{d\delta}{dt} = 0.00001293(\text{S.R.})^2 - 0.00050035(\text{S.R.}) + 0.00469421.$$

These curves intersect the x -axis (axis of S.R.) at 20.6% and at 22.7%. The creep limit of the tested sandwich beams will be found between these intersections:

$$20.6\% \leq \text{S.R.} \leq 22.7\%.$$

Long-term deflection increase

In order to maintain the bending deflection of beams below the admissible value under the long-term loading, the additional deflection produced by the admitted load must be obtained. The sum of the instantaneous deflection (time independent deflection occurred with load application) and the additional deflection by creep gives the long-term deflection. The magnification of bending deflection after t h loading is expressed by what is called the relative creep comparing the instantaneous deflection δ_0 and the total deflection δ_t at t h:

$$\text{Relative creep} = \frac{\delta_t - \delta_0}{\delta_0} (\%). \quad (2)$$

In order to obtain the relative creep at the creep limit, the linear regression analysis was applied. It is needless to say that the relative creep must be null, when the beams are free from load. Therefore, the regression line must pass the original point (0, 0).

Analyzing the first loading data of 9 beams in Fig. 8, its regression line passing the original point is

$$\text{Linear regression: } \frac{\delta_{216} - \delta_0}{\delta_0} = 0.6316 \times \text{S.R.}, \text{ Regression coefficient } R^2 = 0.532.$$

When these beams support the creep limit load (S.R. = 22.1%) over a long period, the bending deflection must be estimated 14.0% larger than the instantaneous deflection δ_0 .

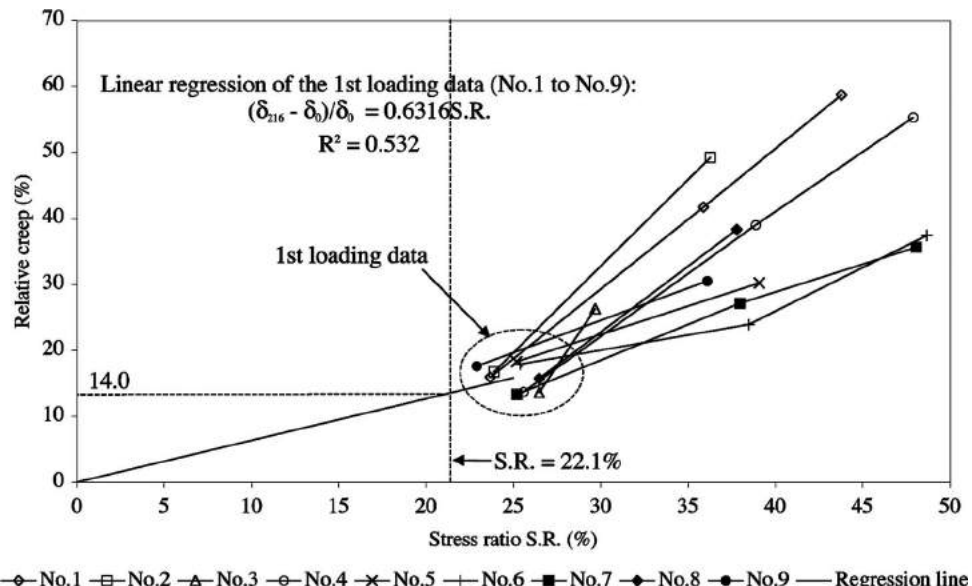


Figure 8. Relationship between relative creep and the stress ratio (9 sandwich beams).

INTERPRETATION OF THE CREEP BEHAVIOUR BY THE BURGER BODY MODEL

This paragraph is devoted to the analytical interpretation of the observed time-dependent behaviour under low-level load by applying the Burger body. The Burger body is a generalized model explaining the creep behaviour by the combination of two Hookean springs and two Newtonian dashpots (Fig. 9) [5]. This model enables the characterization of the complex behaviour simply by four parameters.

The model explains the creep behaviour by the combination of three different deformations indicated in Fig. 10. The total deformation δ is given as

$$\delta = \delta_e + \delta_{de} + \delta_v, \quad (3)$$

$$\delta_e = \frac{P}{k_e}, \quad (4)$$

$$\delta_{de} = \frac{P}{k_{de}} (1 - e^{-t/\tau}), \quad (5)$$

$$\delta_v = \frac{P}{r_v} t, \quad (6)$$

in which δ_e = instantaneous elastic deformation, δ_{de} = delayed elastic deformation (time-dependent elastic deformation), δ_v = viscous deformation (permanent deformation), P = applied load, t = time, k_e = Maxwell's spring constant, k_{de} = Kelvin's spring constant, r_{de} = Kelvin's damping constant, $\tau = r_{de}/k_{de}$ = relaxation-time constant and r_v = Maxwell's damping constant.

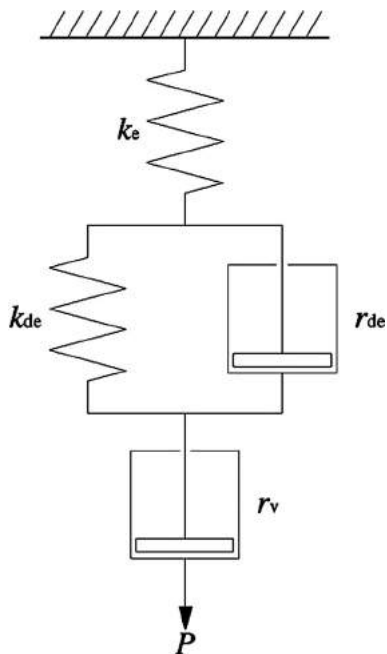


Figure 9. Burger's four-element creep model.

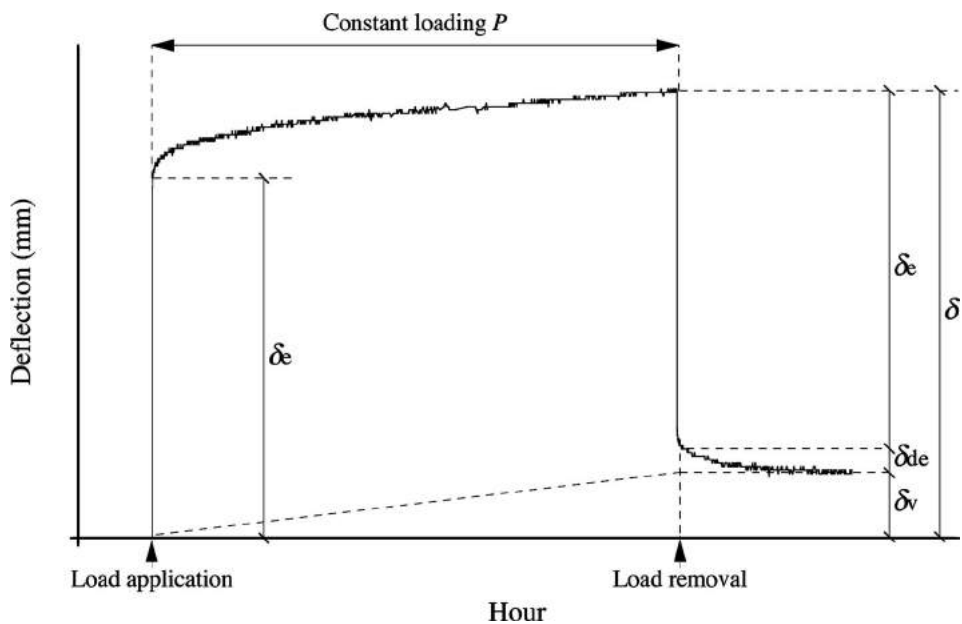


Figure 10. Components of the creep deformation.

Before applying the model for the interpretation of the acquired data, the conditionality must be verified. The Burger body is only valid for the creep with linear viscoelastic behaviour as shown in equations (4)–(6). The linear viscoelasticity can be examined by the comparison of the plural creep curves differing their applied load level. When the proportional relation is found between the load increase and its corresponding deformation increase, the creep behaviour must be linear viscoelastic. Unfortunately, the results of the creep tests did not allow us to observe the linear viscoelastic curves. For example, in Fig. 6, the two curves from the bottom do not show the linear relation. The increase of load between the two curves was too high to confirm the linear viscoelastic behaviour in the first curve. Nevertheless, it can not be asserted that the results of the first loading did not demonstrate the linear viscoelasticity, considering that the applied load level was much lower than the theoretical elastic limit of the beams: 1.71 kN for the poplar beams, 2.55 kN for the sandwich beams (these values were obtained on the basis of published data [6, 7]). The following interpretation is carried out, supposing the beams remained linear viscoelastic during the first loading.

Maxwell's spring constant k_e can be determined by introducing the load and the instantaneous deflection of the beams at $t = 0$ into equation (4). Maxwell's damping constant r_v is given by equation (6) and the permanent deflection. Note that the time introduced in equation (6) must be the time at the removal of the load. The Burger model is not capable to express the gradual recovery of the deformation and simplifies that the permanent deformation appears instantly at the load removal.

Obtaining Kelvin's two constants, k_{de} and τ , needs equation (5) and a pair of deflection-time data. Using the equation twice at times $t = 2$ h and $t = 216$ h, the parameters were computed.

Table 2 shows the necessary experimental data to compute these four constants and Table 3 presents the results of the computation.

The difference between the constants of the poplar beams and those of the sandwich beams in Table 3 explains the influence of the bamboo reinforcement on the creep behaviour. Considering that the applied load on the poplar beams and that on the sandwich beams was almost the same ($P \approx 1.30$ kN), Maxwell's spring constant k_e showed a gain of 12.5% (0.18 to 0.16). This is slightly smaller than the MoE gain computed by using the static values of the specimens listed in Table 1. The lamination theory estimates the average MoE of the sandwich beams as 9769 N/mm² that is about 120% of the average MoE of the poplar beams (8059 N/mm²). This decrease in the spring constant (20% to 12.5%) seems to be due to the increase in moisture content.

Average Maxwell's damping constant r_v of the sandwich beams was 611 kNh/mm, 2.4-times as large as the constant of the poplar beams. A remarkable improvement of recovery ability of the creep deflection by the bamboo reinforcement was confirmed.

As for the Kelvin body, the relaxation-time constant τ showed relatively a small gain. The average constant τ of the sandwich beams was 2.03 h, while that of the

Table 2.

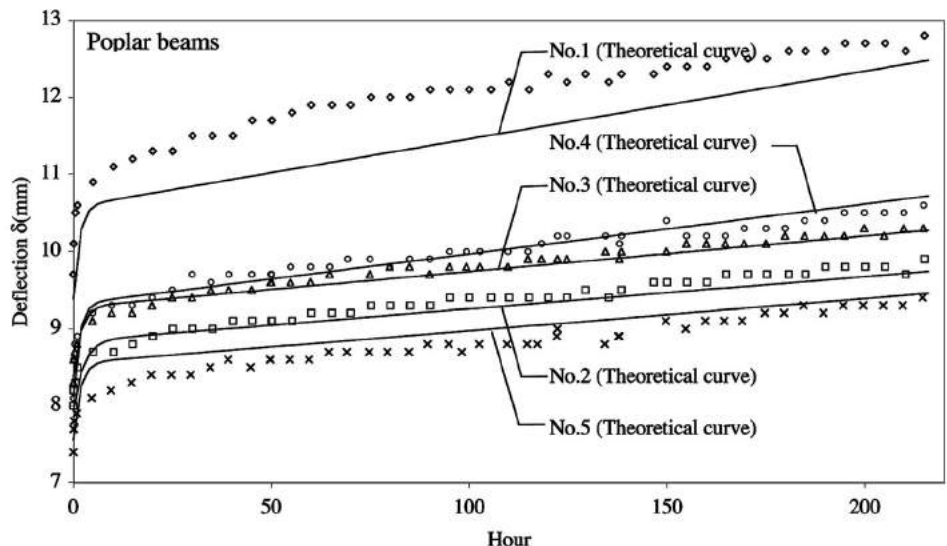
Experimental data necessary for the computation of Burger's constants

	Load (P , kN)	Instantaneous deflection (δ_e , mm)	Point 1		Point 2		Permanent deflection (δ_v , mm)
			t (h)	δ (mm)	t (h)	δ (mm)	
Poplar beams	1	1.22	2	10.6	216	12.8	1.9
	2	1.27	2	8.5	216	9.8	0.9
	3	1.34	2	8.9	216	10.2	1.0
	4	1.38	2	9	216	10.7	1.4
	5	1.36	2	8.1	216	9.3	0.9
Sandwich beams	1	1.26	2	8.6	216	9.5	0.7
	2	1.27	2	7.8	216	8.4	0.3
	3	1.41	2	8.5	216	9.2	0.3
	4	1.36	2	7.6	216	8.3	0.4
	5	1.34	2	7.6	216	8.4	0.6
	6	1.35	2	7.1	216	7.9	0.4
	7	1.34	2	7.7	216	8.5	0.8
	8	1.41	2	8.8	216	9.6	0.7
	9	1.22	2	7.8	216	8.7	0.6

Table 3.

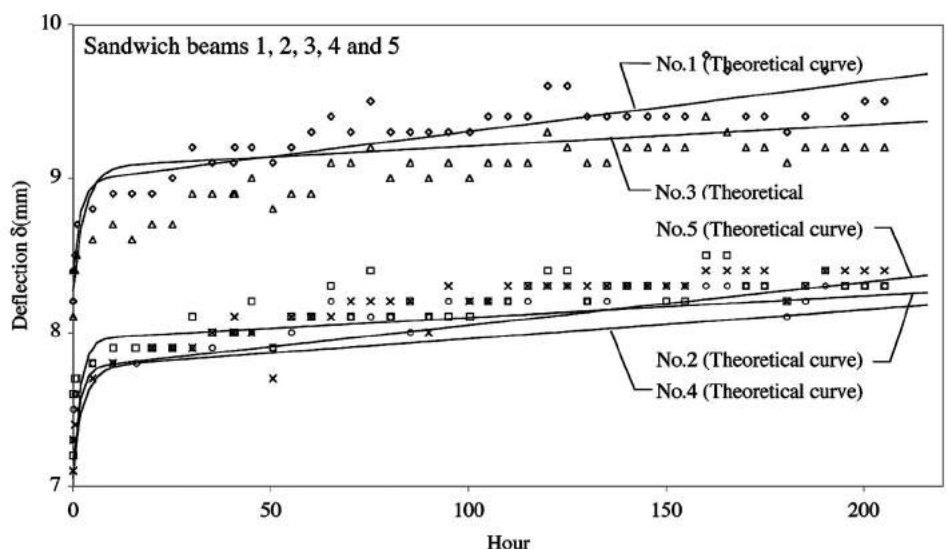
Computed Burger's constants of the tested beams

	Load P (kN)	Maxwell's spring constant (k_e , kN/mm)	Maxwell's damping constant (r_v , kNh/mm)	Kelvin's spring constant (k_{de} , kN/mm)	Relaxation- time constant (τ , h)
Poplar beams	1	1.22	0.13	138.7	1.02
	2	1.27	0.16	304.8	1.41
	3	1.34	0.16	289.4	1.49
	4	1.38	0.17	212.9	1.15
	5	1.36	0.18	326.4	1.36
	Average	1.31	0.16	254.4	1.28
Sandwich beams	1	1.26	0.15	387.9	2.10
	2	1.27	0.18	914.4	1.41
	3	1.41	0.17	1012.3	1.76
	4	1.36	0.19	736.0	2.27
	5	1.34	0.19	483.5	1.92
	6	1.35	0.20	729.0	1.69
	7	1.34	0.18	361.8	6.70
	8	1.41	0.17	435.1	2.35
	9	1.22	0.16	439.2	1.74
	Average	1.33	0.18	611.0	2.44



♦ No.1 (Actual values) □ No.2 (Actual values) ▲ No.3 (Actual values) ○ No.4 (Actual values) × No.5 (Actual values)

Figure 11. Comparison of the actual creep curves to the theoretical curves by the Burger body (poplar beams).



♦ No.1 (Actual values) □ No.2 (Actual values) ▲ No.3 (Actual values) ○ No.4 (Actual values) × No.5 (Actual values)

Figure 12. Comparison of the actual creep curves to the theoretical curves by the Burger body (sandwich beams 1–5).

poplar beams was 1.82 h. The gain was 11.5%. In contrast, average Kelvin's spring constant k_{de} of the sandwich beams gained 91% (2.44 to 1.28). It means that the

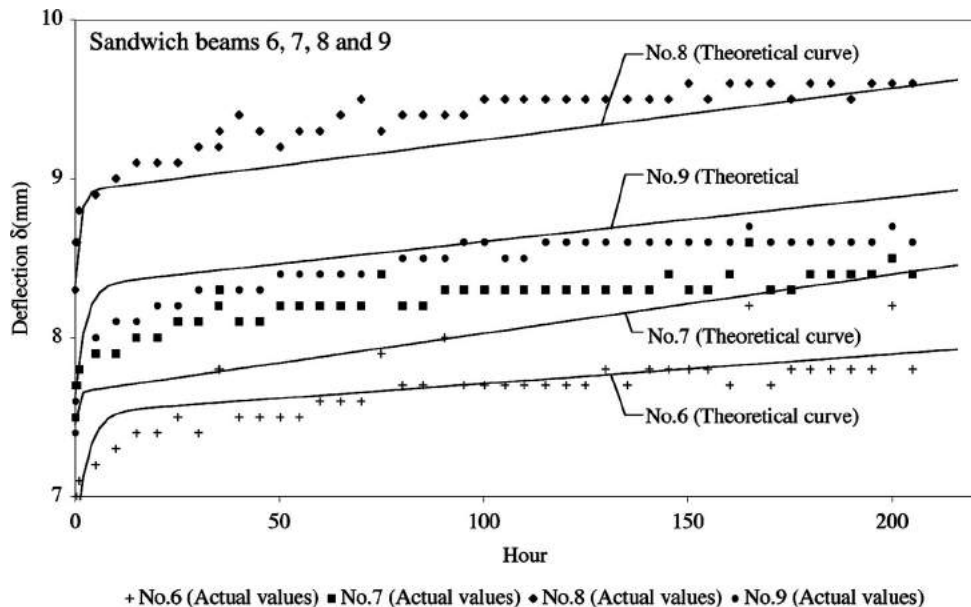


Figure 13. Comparison of the actual creep curves to the theoretical curves by the Burger body (sandwich beams 6–9).

time-dependent deflection δ_{de} of the sandwich beams was about half as large as that of the poplar beams.

Figures 11–13 compare the theoretical creep curves with the actual data of the beams. This comparison shows roughly the correspondence of the theoretical curves with the actual data. Without emphasizing the importance of accuracy, the application of the Burger model seems practical to interpret qualitatively the creep behaviour of the beams during the first loading. This adequacy compensates the supposition of linear viscoelasticity for the incomplete information mentioned previously.

CONCLUSIONS

In order to reveal the efficiency of the bamboo reinforcement under long-term loading, the poplar beams and the sandwich beams were subjected to the creep tests. The results are summarized below.

Analyzing the creep rate evolution by means of a statistical approximation, the creep limit of the sandwich beams was obtained. With the load lower than this level, these beams will not attain the creep failure. The deflection increase of the sandwich beams carrying the load below the creep limit was also estimated.

Describing the creep behaviour by four parameters of the Burger body (two springs and two dashpots), the influence of the bamboo reinforcement was discussed. The comparison of these parameters indicated a remarkable delay and re-

covery of creep deflection by the bamboo reinforcement. It must be noted that both types of beams were tested with the same amount of load and compared disregarding the difference in static bending strength of each material. The adequacy of this comparison is open to question. The long-term behaviour at the same stress ratio remains to be studied.

In addition to the above-mentioned question about the loading condition, the next step is to test an adequate number of large scale specimens for the discussion about the statistical reliability of the performance.

Acknowledgements

This research project was directed by Prof. J. Natterer and Dr. P. Navi, Swiss Federal Institute of Technology Lausanne, and financed by the Swiss National Science Foundation.

REFERENCES

1. Y. Amino, Conception and feasibility of bamboo — precocious wood composite beams, *Journal of Bamboo and Rattan* **2** (3), 261–279 (2003).
2. Y. Amino, Bamboo-precocious wood composite beams: Theoretical prediction of the bending behavior, *Journal of Bamboo and Rattan* **3** (2), 107–122 (2004).
3. J. Mukudai and M. Taguchi, Non-linear viscoelastic behavior and non-linear superposition of wood in bending. I. Non-linear creep behavior and evaluation of stepped-load creep deflection at non-linear stress level, *Mokuzai Gakkaishi* **26** (3), 146–158 (1980).
4. Japanese Standards Association, *JIS Handbook 24-2*. Japanese Standards Association, Tokyo (1998) (in Japanese).
5. J. Bodig and B. A. Jayne, *Mechanics of Wood and Wood Composites*, reprint edition. Krieger, Malabar, FL (1993).
6. Ringyo Shikenjo, *Mokuzai Kogyo Handbook*. Maruzen, Tokyo (1982) (in Japanese).
7. J. Sell and F. Kropf, *Propriété et Caractéristiques des Essences de Bois*. Lignum, Zurich (1989).

Copyright of Journal of Bamboo & Rattan is the property of VSP International Science Publishers and its content may not be copied or emailed to multiple sites or posted to a listserv without the copyright holder's express written permission. However, users may print, download, or email articles for individual use.